Identification of a novel cationic glycolipid in *Streptococcus agalactiae* that contributes to brain entry and meningitis

Luke R. Joyce[a], Haider S. Manzer[b], Jéssica da C. Mendonça[b,c], Ricardo Villarreal[b], Prescilla E. Nagao[c] , Kelly S. Doran[b#,] Kelli L. Palmer[a#], and Ziqiang Guan[d#]

[a]Department of Biological Sciences, The University of Texas at Dallas, Richardson, TX, 75080

[b]Department of Immunology and Microbiology, University of Colorado School of Medicine, Aurora, CO, 80045

[c]Rio de Janeiro State University, Roberto Alcântara Gomes Biology Institute, Rio de Janeiro, RJ, Brazil

[d]Department of Biochemistry, Duke University Medical Center, Durham, NC, 27710

Short title: GBS MprF synthesizes a novel glycolipid that contributes to meningitis

#Corresponding authors

Kelly S. Doran: Kelly.Doran@CUAnschutz.edu

Kelli L. Palmer: Kelli.Palmer@UTDallas.edu

Ziqiang Guan: Ziqiang.Guan@Duke.edu

Keywords: Group B *Streptococcus*, Lipidomics, Glycolipid, Meningitis, MprF

Abstract

Bacterial membrane lipids are critical for membrane bilayer formation, cell division, protein localization, stress responses, and pathogenesis. Despite their critical roles, membrane lipids have not been fully elucidated for many pathogens. Here, we report the discovery of a novel cationic glycolipid, Lysyl-Glucosyl-Diacylglycerol (Lys-Glc-DAG) that is synthesized in high abundance by the bacterium *Streptococcus agalactiae* (Group B *Streptococcus*, GBS). To our knowledge, Lys-Glc-DAG is more positively charged than any other known lipids. Lys-Glc-DAG carries two positive net charges per molecule, distinct from the widely described lysylated phospholipid Lysyl-phosphatidylglycerol (Lys-PG) which carries one positive net charge due to the presence of a negatively charged phosphate moiety. We use normal phase liquid chromatography (NPLC) coupled with electrospray ionization (ESI) high-resolution tandem mass spectrometry (HRMS/MS) and genetic approaches to determine that Lys-Glc-DAG is synthesized by the enzyme MprF in GBS, which covalently modifies the neutral glycolipid Glc-DAG with the cationic amino acid lysine. GBS is a leading cause of neonatal meningitis, which requires traversal of the endothelial blood-brain barrier (BBB). We demonstrate that GBS strains lacking *mprF* exhibit a significant decrease in the ability to invade BBB endothelial cells. Further, mice challenged with a GBSΔ*mprF* mutant developed bacteremia comparably to Wild-Type infected mice yet had less recovered bacteria from brain tissue and a lower incidence of meningitis. Thus, our data suggest that Lys-Glc-DAG may contribute to bacterial uptake into host cells and disease progression. Importantly, our discovery provides a platform for further study of cationic lipids at the host-pathogen interface.

Introduction

Bacterial cellular membranes are dynamic structures that are critical for survival under varying environmental conditions and are essential for host-pathogen interactions. Phospholipids and glycolipids within the membrane have varying chemical properties that alter the physiology of the membrane, which bacteria can modulate in response to environmental stresses such as pH (1), antibiotic treatment (2), and human metabolites (3). Despite their critical roles in the survival and pathogenesis, membrane lipids have not been carefully characterized using modern lipidomic techniques for many important human pathogens, including *Streptococcus agalactiae* (Group B *Streptococcus*; GBS). GBS colonizes the lower genital and gastrointestinal tracts of ~30% of healthy women (4, 5). However, GBS can cause sepsis and pneumonia in newborns and is a leading cause of neonatal meningitis, resulting in long-lasting neurological effects in survivors (6-8). Due to the severity of the resulting diseases, intrapartum antibiotic prophylaxis is prescribed for colonized pregnant women (7, 9). Even with these measures, a more complete understanding of GBS pathogenesis and new therapeutic and preventive measures are needed to mitigate the devastating impact of GBS neonatal infection.

Research on the pathogenesis of the GBS has mainly focused on cell wall-anchored or secreted proteins and polysaccharides that aid in the attachment to and invasion of host cells. The numerous attachment and virulence factors possessed by the GBS are summarized in a recent review by Armistead *et al* 2019 (10). Comparatively little is known about GBS cellular membrane lipids. To our knowledge, the only characterization of GBS lipids prior to our current study was the identification of the phospholipids

phosphatidylglycerol (PG), cardiolipin (CL), and lysyl-phosphatidylglycerol (Lys-PG) in GBS (11, 12). Similarly, investigation into the glycolipids of the GBS membrane has focused on di-glucosyl-diacylglycerol (Glc_2-DAG), which is the lipid anchor of the Type I lipoteichoic acid, and its role in pathogenesis (13).

In this study, we utilized normal phase liquid chromatography (NPLC) coupled with electrospray ionization (ESI) high-resolution tandem mass spectrometry (HRMS/MS) to characterize the GBS membrane lipid composition, and identified a novel cationic glycolipid, lysyl-glucosyl-diacylglycerol (Lys-Glc-DAG), which comprises a major portion of the GBS total lipid extract. While Lys-PG has been reported in a range of bacterial species (14), Lys-Glc-DAG represents, to our knowledge, the first example of lysine modification of a neutral glycolipid. By gene deletion and heterologous expression, we show the GBS MprF enzyme is responsible for the biosynthesis of both the novel Lys-Glc-DAG and Lys-PG. Most strikingly, using an *in vivo* hematogenous murine infection model, we demonstrate that MprF does not contribute to GBS bloodstream survival. This distinguishes the GBS MprF from the well-known *Staphylococcus aureus* MprF, which synthesizes only Lys-PG (15, 16). Rather, GBS MprF contributes specifically to meningitis and penetration of the blood-brain barrier. These results greatly expand our knowledge of naturally occurring lipids and MprF functionality and reveal insights into the pathogenesis of meningitis caused by GBS.

Results

Identification of Lys-Glc-DAG, a novel cationic glycolipid in GBS

The membrane lipids of three GBS clinical isolates of representative serotypes were characterized: COH1 (17), A909 (18), CNCTC 10/84 and CJB111 (serotypes III, 1a, and V, respectively) (19). Common Gram-positive bacterial lipids were identified by normal phase LC coupled with negative ion ESI/MS/MS, including diacylglycerol (DAG), monohexosyldiacylglycerol (MHDAG), dihexosyldiacylglycerol (DHDAG), phosphatidylglycerol (PG), and lysyl-phosphatidylglycerol (Lys-PG), as shown by the negative total ion chromatogram (TIC) (Fig. 1A).

Surprisingly, the positive TIC (Fig. 1B, Supplemental Figure S1) shows highly abundant peaks of unknown identity at the retention time ~25-29 min. The mass spectra (Fig. 1C) and LC retention times of this lipid do not match with any other bacterial lipids we have analyzed or exact masses in lipidomic databases. Tandem MS (MS/MS) in the positive ion mode (Fig. 1D), negative ion mode (Fig. 1E), and high-resolution mass measurement (Fig. 1C) allowed us to propose lysyl-glucosyl-diacylglycerol (Lys-Glc-DAG) (Fig. 1F) as the structure of this unknown lipid. Observed and exact masses of Lys-Glc-DAG are shown in Table S1. The assignment of glucose was based on the observation that glucosyl-diacylglycerol (Glc-DAG) is a major membrane component of GBS and other streptococci (13), and results from an isotopic labeling experiment using ^{13}C-labeled glucose (Glucose-$^{13}C_6$). The assignment of lysine modification was supported by an isotopic labeling experiment with deuterated lysine (lysine-*d4*). The expected mass shifts (+4 Da) were observed in both molecular ions and MS/MS product ions (Supplemental Figure S2). Comparison of both MS/MS spectra of labeled (Glucose-$^{13}C_6$) and unlabeled Lys-Glc-DAG indicates the lysine residue is linked to the 6-position of glucose

(Supplemental Figure S2). Lys-Glc-DAG consists of several molecular species with different fatty acyl compositions resulting in different retention times and multiple, unresolved TIC peaks (~25-29 min).

GBS MprF synthesizes Lys-Glc-DAG

The enzyme MprF (multiple peptide resistance factor) catalyzes the aminoacylation of PG with lysine in some Gram-positive pathogens (15, 20). We determined that GBS MprF is responsible and sufficient for synthesizing Lys-Glc-DAG as well as Lys-PG. Deletion of *mprF* from both COH1 and CJB111 abolishes Lys-Glc-DAG and Lys-PG synthesis, which are restored by complementation (Fig. 1G, Supplemental Figure S3). Deletion of GBS *mprF* does not confer a growth defect in Todd-Hewitt broth or tissue culture medium. The oral colonizer *Streptococcus mitis* does not encode *mprF* or synthesize Lys-PG but synthesizes Glc-DAG and PG (2, 3). Heterologous expression of GBS *mprF* in *S. mitis* results in Lys-Glc-DAG and Lys-PG production (Fig. 1H), while expression of *Enterococcus faecium mprF* results in only Lys-PG production (Fig. 1H), as expected (1). Biosynthetic pathways involving MprF are shown in Fig. 1I.

MprF contributes to GBS pathogenesis

We investigated whether MprF contributes to GBS invasion into brain endothelial cells and development of meningitis. To mimic the human blood-brain barrier (BBB), we utilized the human cerebral microvascular endothelial cell line hCMEC/D3. *In vitro* assays for adhesion and invasion were performed as described previously (13, 21, 22). There was no significant difference in the ability of Δ*mprF* compared to WT and complement cells to

attach to hCMEC/D3 cells (Fig. 2A). However, we observed a significant decrease in the amount of Δ*mprF* recovered from the intracellular compartment of hCMEC/D3 cells (Fig. 2A). The reduced invasion phenotype was confirmed in the hypervirulent serotype V strain, CJB111 (23, 24) (Supplemental Figure S4). Intracellular survival requires GBS to survive low pH conditions in lysosomes (pH 4.5 – 5.5) (25), and Δ*mprF* is unable to survive low pH conditions (Fig. 2B). This suggests that MprF promotes GBS invasion and possibly intracellular survival in brain endothelial cells.

We hypothesized that these *in vitro* phenotypes of Δ*mprF* would translate into a diminished ability to penetrate the BBB and produce meningitis *in vivo*. Using our standard model of GBS hematogenous meningitis (13, 21) mice were challenged with either WT GBS or Δ*mprF*. Mice were sacrificed at 72 h to determine bacterial loads in blood and brain tissue. We recovered significantly less CFU in the brains of Δ*mprF*-infected mice compared to the WT-infected mice (Fig. 2C). However, there was no significant difference in CFU recovered from the bloodstream (Fig. 2D), demonstrating that Δ*mprF* does not have a general *in vivo* growth defect. Furthermore, mice challenged with WT GBS had significantly more leukocyte infiltration, meningeal thickening and neutrophil chemokine, KC, in brain homogenates compared to Δ*mprF* mutant-infected animals (Fig. 2E-G). Taken together, *mprF* contributes to GBS penetration into the brain and to the pathogenesis of meningitis *in vivo*.

Discussion

Lipid nanoparticles are essential for mRNA vaccine delivery. Engineered cationic lipids are utilized in lipid nanoparticles for vaccine and drug delivery and are required for uptake of particles into cells (26, 27). Substantial effort has been dedicated to the synthesis of cationic lipids with low toxicity and efficient delivery properties. Here, we report the discovery of Lys-Glc-DAG, a naturally occurring cationic glycolipid synthesized in high abundance by GBS, which in conjunction with Lys-PG aids in invasion of human endothelial cells. We discovered that GBS MprF uniquely synthesizes the novel and highly abundant Lys-Glc-DAG, as well as Lys-PG. This establishes that GBS capitalizes on MprF to modulate charges of both glycolipids and phospholipids at the membrane.

MprF catalyzes the aminoacylation of the anionic phospholipid PG in a range of Gram-positive and Gram-negative bacteria (15, 20). MprF is a membrane-bound enzyme comprised of a N-terminal lipid flippase domain (28) and a C-terminal catalytic domain that catalyzes the aminoacylation of the glycerol group of PG by using aminoacyl-tRNAs as the amino acid donors (29-31). An important function of PG aminoacylation is proposed to be lowering the net negative charge of the cellular envelope to confer protection from cationic antimicrobial peptides (CAMPs) produced by host immune systems and bacteriocins produced by competitor bacteria (15, 20). However, a previous study observed no contribution of *mprF* to GBS *in vitro* susceptibility to commonly studied CAMPs, which is unlike the well-characterized *S. aureus mprF* (32), thus highlighting the unique differences between the extracellular surface of these bacteria.

Based on our tissue culture and mouse infection experiments, we propose that GBS have an MprF enzyme and corresponding cellular lipid properties that are adapted for efficient invasion of mammalian cells. Deletion of *mprF* impacts GBS virulence, but only for meningitis, and not for bacteremia. This demonstrates that MprF plays a specific role in BBB penetration, but not *in vivo* survival in general. It is unknown how lysinylated lipids in the GBS membrane, which is covered by a layer of peptidoglycan, mechanistically impact invasion. Because Lys-Glc-DAG is abundantly synthesized by GBS MprF, with Lys-PG a comparatively minor product, it is likely that Lys-Glc-DAG is the most relevant lipid for meningitis pathogenesis. Speculatively, Lys-Glc-DAG may contribute to membrane vesicle (MV) formation by GBS. MVs have previously been shown to be pro-inflammatory and result in preterm birth and fetal death in mice (33), but have not been studied during meningitis progression. In future studies, it will be key to investigate this, as well as the specific host inflammatory and signaling responses to the GBS *mprF* mutant.

Our identification of the novel Lys-Glc-DAG glycolipid rationalizes further study of the lipidomes of human pathogens. First, lipids contribute to virulence, and understanding these virulence mechanisms and the mechanisms for lipid synthesis may identify novel antimicrobial drug targets. The decreased *in vivo* pathogenicity of the Δ*mprF* mutant identifies GBS MprF as a candidate for targeting by antimicrobial strategies. Moreover, Lys-Glc-DAG could be utilized as a specific molecular biomarker for GBS diagnostics. Second, pathogens use lipids to modulate their surface charges and interact with their hosts, and they innovate lipids to meet their specific needs. Lys-Glc-DAG is a naturally

206 occurring, strongly cationic lipid with potential for use in lipid nanoparticles for vaccine
207 and drug delivery. Importantly, our discovery suggests that lipidome analysis of human
208 pathogens is likely to reveal novel lipids of biotechnological utility.
209
210 **Materials and methods**
211 **Bacterial strains, media, and growth conditions**
212 See Table S2 for strains used in this study. GBS strains were grown statically at 37°C in
213 Todd-Hewitt Broth (THB) and *S. mitis* strains were grown statically at 37°C and 5% CO_2,
214 unless otherwise stated. Streptococcal chemically defined medium (34) was diluted from
215 stock as described (35) with 1% w/v glucose (referred to as DM), slightly modified from
216 (36), unless otherwise stated. *Escherichia coli* strains were grown in Lysogeny Broth (LB)
217 at 37°C with rotation at 225 rpm. Kanamycin and erythromycin (Sigma-Aldrich) were
218 supplemented to media at 50 µg/mL and 300 µg/mL for *E. coli,* respectively, or 300 µg/mL
219 and 5 µg/mL, respectively, for streptococcal strains.
220
221 **Routine molecular biology techniques**
222 All PCR reactions utilized Phusion polymerase (Thermo Fisher). PCR products and
223 restriction digest products were purified using GeneJET PCR purification kit (Thermo
224 Fisher) per manufacturer protocols. See Table S3 for primers. Plasmids were extracted
225 using GeneJET plasmid miniprep kit (Thermo Fisher) per manufacturer protocols.
226 Restriction enzyme digests utilized XbaI, XhoI, and PstI (New England Biolabs) for 3 h at
227 37°C in a water bath. Ligations utilized T4 DNA ligase (New England Biolabs) at 16°C
228 overnight or Gibson Assembly Master Mix (New England Biolabs) per manufacturer

229 protocols where stated. All plasmid constructs were sequence confirmed by Sanger
230 sequencing (Massachusetts General Hospital DNA Core or CU Anschutz Molecular
231 Biology Core).
232
233 **Deuterated lysine and $^{13}C_6$-D-glucose isotope tracking**
234 A GBS COH1 colony was inoculated into 15 mL of DM containing 450 µM lysine-*d4*
235 (Cambridge Isotopes Laboratories) or a single COH1 colony was inoculated into 10 mL
236 DM supplemented with 0.5% w/v $^{13}C_6$D-glucose (U-13C6, Cambridge Isotopes
237 Laboratories) for overnight growth for lipidomic analysis described below.
238
239 **Construction of MprF expression plasmids**
240 Genomic DNA was isolated using the Qiagen DNeasy Blood and Tissue kit per the
241 manufacturer's protocol with the exception that cells were pre-treated with 180 µL 50
242 mg/mL lysozyme, 25 µL 2500 U/mL mutanolysin, and 15 µL 20 mg/mL pre-boiled RNase
243 A and incubated at 37°C for 2 h. The *mprF* genes from GBS COH1, (GBSCOH1_1931),
244 GBS CJB111 (ID870_10050), and *E. faecium* 1,231,410 (EFTG_00601) were amplified
245 and either Gibson ligated into pABG5Δ*phoZ* (37) or ligated into pDCErm (38). Plasmid
246 constructs were transformed into chemical competent *E. coli*. Briefly, chemically
247 competent cells were incubated for 10 min on ice with 5 µL of Gibson reaction before heat
248 shock at 42°C for 70 sec, then placed on ice for 2 min before 900 µL of cold SOC medium
249 was added. Outgrowth was performed at 37°C, with shaking at 225 rpm, for 1 h. Cultures
250 were plated on LB agar plates containing 50 µg/mL kanamycin. Colonies were screened
251 by PCR for presence of the *mprF* insert.

252

253 **Expression of *mprF* in *S. mitis***

254 Natural transformation was performed as previously described (3). Briefly, precultures
255 were thawed at room temperature, diluted in 900 µL of THB, further diluted 1:50 in
256 prewarmed 5 mL THB, and incubated for 45 min at 37°C. 500 µL of culture was then
257 aliquoted with 1 µL of 1 mg/ml competence-stimulating peptide (EIRQTHNIFFNFFKRR)
258 and 1 µg/mL plasmid. Transformation reaction mixtures were cultured for 2 h at 37°C in
259 microcentrifuge tubes before being plated on THB agar supplemented with 300 µg/mL
260 kanamycin. Single transformant colonies were cultured in 15 mL THB overnight. PCR
261 was used to confirm the presence of the *mprF* insert on the plasmid. Plasmids were
262 extracted and sequence confirmed as described above. Lipidomics was performed as
263 described below in biological triplicate.

264

265 **Construction of *mprF* deletion plasmids**

266 Regions ~2 kb upstream and downstream of the GBS COH1 *mprF* (GBSCOH1_1931) or
267 CJB111 (ID870_10050) were amplified using PCR. Plasmid, pMBSacB (39), and the
268 PCR products were digested using appropriate restriction enzymes and ligated overnight.
269 7 µL of the ligation reaction was transformed into chemically competent *E. coli* DH5α as
270 described above, except that outgrowth was performed at 28°C with shaking at 225 rpm
271 for 90 min prior to plating on LB agar supplemented with 300 µg/mL erythromycin. Plates
272 were incubated at 28°C for 72 h. Colonies were screened by PCR for correct plasmid
273 construction. Positive colonies were inoculated into 50 mL LB media containing antibiotic
274 and incubated at 28°C with rotation at 225 rpm for 72 h. Cultures were pelleted using a

Sorvall RC6+ centrifuge at 4,280 x *g* for 6 min at room temperature. Plasmid was extracted as described above except the cell pellet was split into 5 columns to prevent overloading and serial eluted into 50 µL. Plasmid construction was confirmed via restriction digest using XhoI and XbaI, and the insert was PCR amplified and sequence-verified.

Generation of electrocompetent GBS cells for *mprF* knockout

Electrocompetent cells were generated as described (39) with minor modifications. Briefly, a GBS COH1 or CJB111 colony was inoculated in 5 mL M17 medium (BD Bacto) with 0.5% glucose and grown overnight at 37°C. The 5 mL was used to inoculate a second overnight culture of 50 mL pre-warmed filter-sterilized M17 medium containing 0.5% glucose, 0.6% glycine, and 25% PEG 8000. The second overnight was added to 130 mL of the same medium and grown for 1 h at 37°C. Cells were pelleted at 3,200 x *g* in a Sorvall RC6+ at 4°C for 10 min. Cells were washed twice with 25 mL cold filter-sterilized GBS wash buffer containing 25% PEG 8000 and 10% glycerol in water, and pelleted as above. Cell pellets were re-suspended in 1 mL GBS wash buffer and either used immediately for transformation or stored in 100 µL aliquots at -80°C until use.

Deletion of GBS COH1 and CJB111 *mprF*

Electrocompetent cells were generated as described (39) with minor modifications. The double crossover homologous recombination knockout strategy was performed as described previously (22, 39, 40) with minor modifications. 1 µg of plasmid was added to electrocompetent GBS cells and transferred to a cold 1 mm cuvette (Fisher or BioRad).

298 Electroporation was carried out at 2.5 kV on an Eppendorf eporator. 1 mL of THB
299 containing 12.5% PEG 8000, 20 mM $MgCl_2$, and 2 mM $CaCl_2$ was immediately added
300 and then the entire reaction was transferred to a glass culture tube. Outgrowth was at
301 28°C for 2 h followed by plating on THB agar supplemented with 5 µg/mL erythromycin.
302 Plates were incubated for 48 h at 28°C. A single colony was cultured overnight in 5 mL
303 THB with 5 µg/mL erythromycin at 28°C. The culture was screened via PCR for the
304 plasmid insert with the initial denaturing step extended to 10 min. The overnight culture
305 was diluted 1:1000 THB containing 5 µg/mL erythromycin and incubated overnight at
306 37°C to promote single cross over events. The culture was then serial diluted and plated
307 on THB agar plates with antibiotic and incubated at 37°C overnight. Colonies were
308 screened for single crossover events by PCR. Single crossover colonies were inoculated
309 in 5 mL THB at 28°C to promote double crossover events. Overnight cultures were diluted
310 1:1000 into 5 mL THB containing sterile 0.75 M sucrose and incubated at 37°C. Overnight
311 cultures were serial diluted and plated on THB agar and incubated at 37°C overnight.
312 Colonies were patched onto THB agar with and without 5 µg/mL erythromycin to confirm
313 loss of plasmid. Colonies were also screened by PCR for the loss of *mprF*. Colonies
314 positive for the loss of *mprF* were inoculated into 5 mL THB at 37°C. Cultures were
315 stocked and gDNA extracted as described above, with minor modifications. Sequence
316 confirmation of the *mprF* knockout was done via Sanger sequencing (Massachusetts
317 General Hospital DNA Core or CU Anschutz Molecular Biology Core). The mutant was
318 grown overnight in 15 mL THB at 37°C and pelleted at 6,150 x *g* for 5 min in a Sorvall
319 RC6+ centrifuge at room temperature for lipid extraction as described. Genomic DNA of
320 COH1Δ*mprF* was isolated as described above and whole genome sequencing was

performed in paired-end reads (2 by 150 bp) on the Illumina NextSeq 550 platform at the Microbial Genome Sequencing Center (Pittsburgh, PA). Illumina sequence reads are deposited in the Sequence Read Archive, accession PRJNA675025.

Complementation of *mprF* in COH1Δ*mprF* and CJB111Δ*mprF*

Electrocompetent GBS strains were generated as previously described (41). Briefly, GBSΔ*mprF* was inoculated into 5 mL THB with 0.6% glycine and grown overnight. The culture was expanded to 50 mL in pre-warmed THB with 0.6% glycine and grown to an OD_{600} nm of 0.3 and pelleted for 10 min at 3200 x *g* at 4°C in a Sorvall RC6+ floor centrifuge. The pellet was kept on ice through the remainder of the protocol. The pellet was washed twice with 25 mL and once with 10 mL of cold 0.625 M sucrose and pelleted as above. The cell pellet was resuspended in 400 µL of cold 20% glycerol, aliquoted in 50 µL aliquots, and used immediately or stored at -80°C until use. Electroporation was performed as described above, with recovery in THB supplemented with 0.25 M sucrose, and plated on THB agar with kanamycin at 300 µg/mL.

Acidic Bligh-Dyer extractions

Centrifugation was performed using a Sorvall RC6+ centrifuge. Cultures were pelleted at 4,280 x *g* for 5 min at room temperature unless otherwise stated. The supernatants were removed, and cell pellets were stored at -80°C until acidic Bligh-Dyer lipid extractions were performed as described (3). Briefly, cell pellets were resuspended in 1X PBS (Sigma-Aldrich) and transferred to Coring Pyrex glass tubes with PTFR-lined caps (VWR), followed by 1:2 vol:vol chloroform:methanol addition. Single phase extractions

were vortexed periodically and incubated at room temperature for 15 minutes before 500 x *g* centrifugation for 10 min. A two-phase Bligh-Dyer was achieved by addition of 100 µL 37% HCl, 1 mL $CHCl_3$, and 900 µl of 1X PBS, which was then vortexed and centrifuged for 5 min at 500 x *g.* The lower phase was removed to a new tube and dried under nitrogen before being stored at -80°C prior to lipidomic analysis.

Liquid Chromatography/Electrospray Ionization Mass Spectrometry

Normal phase LC was performed on an Agilent 1200 quaternary LC system equipped with an Ascentis silica HPLC column (5 µm; 25 cm by 2.1 mm; Sigma-Aldrich) as described previously (42, 43). Briefly, mobile phase A consisted of chloroform-methanol-aqueous ammonium hydroxide (800:195:5, vol/vol), mobile phase B consisted of chloroform-methanol-water-aqueous ammonium hydroxide (600:340:50:5, vol/vol), and mobile phase C consisted of chloroform-methanol-water-aqueous ammonium hydroxide (450:450:95:5, vol/vol). The elution program consisted of the following: 100% mobile phase A was held isocratically for 2 min, then linearly increased to 100% mobile phase B over 14 min, and held at 100% mobile phase B for 11 min. The LC gradient was then changed to 100% mobile phase C over 3 min, held at 100% mobile phase C for 3 min, and, finally, returned to 100% mobile phase A over 0.5 min and held at 100% mobile phase A for 5 min. The LC eluent (with a total flow rate of 300 µl/min) was introduced into the ESI source of a high-resolution TripleTOF5600 mass spectrometer (Sciex, Framingham, MA). Instrumental settings for negative-ion ESI and MS/MS analysis of lipid species were: IS = -4,500 V, CUR = 20 psi, GSI = 20 psi, DP = -55 V, and FP = -150V. Settings for positive-ion ESI and MS/MS analysis were: IS = +5,000 V, CUR = 20 psi, GSI

= 20 psi, DP = +55 V, and FP = +50V. The MS/MS analysis used nitrogen as the collision gas. Data analysis was performed using Analyst TF1.5 software (Sciex, Framingham, MA).

pH-adjusted THB growth

Approximately 30 mL of fresh THB were adjusted to different pH values, measured using a Mettler Toledo FiveEasy pH/MV meter, and sterile-filtered using 0.22 µM syringe filters. A final volume of 200 µL culture medium was aliquoted per well in a flat-bottom 96 well plate (Falcon); culture media were not supplemented with antibiotics. Overnight cultures of GBS strains were used to inoculate the wells to a starting OD_{600nm} 0.02 per well. Plates were incubated for 24 h at 37°C before OD_{600nm} was read using a BioTek MX Synergy 2 plate reader. This experiment was performed in biological triplicate.

hCMEC cell adherence and invasion assays

Human Cerebral Microvascular Endothelial cells hCMEC/D3 (obtained from Millipore) were grown in EndoGRO-MV complete media (Millipore, SCME004) supplemented with 5% fetal bovine serum (FBS) and 1 ng/ml fibroblast growth factor-2 (FGF-2; Millipore). Cells were grown in tissue culture treated 24 well plates and 5% CO_2 at 37°C.

Assays to determine the total number of bacteria adhered to host cells or intracellular bacteria were performed as described previously (21, 22). Briefly, bacteria were grown to mid log phase (OD_{600nm} 0.4-0.5) and normalized to 1 x 10^8 to infect cell monolayers at a multiplicity of infection (MOI) of 1 (1 x 10^5 CFU per well). The total cell-associated GBS

were recovered after 30 min incubation. Cells were washed slowly five times with 500 µL 1X PBS (Sigma) and detached by addition of 100 µL of 0.25% trypsin-EDTA solution (Gibco) and incubation for 5 min before lysing the eukaryotic cells with the addition of 400 µL of 0.025% Triton X-100 (Sigma) and vigorous pipetting. The lysates were then serially diluted and plated on THB agar and incubated overnight to determine CFU. Bacterial invasion assays were performed as described above except infection plates were incubated for 2 h before incubation with 100 µg gentamicin (Sigma) and 5 µg penicillin (Sigma) supplemented media for an additional 2 h to kill all extracellular bacteria, prior to being trypsinized, lysed, and plated as described. Experiments were performed in biological triplicate with four technical replicates per experiment.

Murine model of GBS hematogenous meningitis

All animal experiments were conducted under the approval of the Institutional Animal Care and Use Committee (#00316) at the University of Colorado Anschutz Medical Campus and performed using accepted veterinary standards. The murine meningitis model was performed as previously described (22, 44, 45). Briefly, 7-week-old male CD1 (Charles River) mice were challenged intravenously with 1×10^9 CFU of WT COH1 or the isogenic Δ*mprF* mutant. At 72 h post-infection, mice were euthanized and blood and brain tissue were harvested, homogenized, and serially diluted on THB agar plates to determine bacterial CFU.

Histology and ELISA

412 Mouse brain tissue was frozen in OCT compound (Sakura) and sectioned using a
413 CM1950 cryostat (Leica). Sections were stained using hematoxylin and eosin (Sigma)
414 and images were taken using a BZ-X710 microscope (Keyence). Images were analyzed
415 using ImageJ software. Meningeal thickening was quantified from sections taken from
416 three different mice per group, and six images per slide. Meningeal thickening was
417 quantified across two points per image. KC protein from mouse brain homogenates was
418 detected by enzyme-linked immunosorbent assay according to the manufacturer's
419 instructions (R&D systems).
420

421 **Conflict of interest**

422 The authors have declared that no conflict of interest exists.
423

424 **Acknowledgements**

425 We thank Kathryn Patras at the University of California San Diego for the CNCTC 10/84
426 strain and Moutusee Islam in Kelli Palmer's lab at The University of Texas at Dallas for
427 *E. faecium* 1,231,410 DNA.
428

429 The work was supported in part by T32 5T32AI052066-18 and F31 AI164674 for H.S.M,
430 the Coordenação de Aperfeiçoamento de Pessoal de Nível Superior, Brazil (CAPES;
431 finance code 001 to J.D.C.M), by grants R01NS116716 and R01AI153332 from the
432 National Institutes of Health (NIH) to K.S.D and associated NIH/NINDS supplement from
433 R01NS116716 to R.V, NIH grant R21AI130666 and the Cecil H. and Ida Green Chair in

Systems Biology Science to K.P, NIH grant R56AI139105 to K.P and Z.G, and NIH grant U54GM069338 to Z.G.

References

1. Roy H. Tuning the properties of the bacterial membrane with aminoacylated phosphatidylglycerol. IUBMB Life. 2009;61:940-53.
2. Adams HM, Joyce LR, Guan Z, Akins RL, Palmer KL. *Streptococcus mitis* and *S. oralis* Lack a Requirement for CdsA, the Enzyme Required for Synthesis of Major Membrane Phospholipids in Bacteria. Antimicrobial agents and chemotherapy. 2017;61:e02552-16.
3. Joyce LR, Guan Z, Palmer KL. Phosphatidylcholine Biosynthesis in Mitis Group Streptococci via Host Metabolite Scavenging. Journal of bacteriology. 2019;201:e00495-19.
4. Wilkinson HW. Group B Streptococcal Infection in Humans. Annual Review of Microbiology. 1978;32:41-57.
5. Doran KS, Nizet V. Molecular pathogenesis of neonatal Group B Streptococcal infection: No longer in its infancy. Molecular Microbiology. 2004;54:23-31.
6. Hall J, Adams NH, Bartlett L, Seale AC, Lamagni T, Bianchi-Jassir F, et al. Maternal Disease With Group B *Streptococcus* and Serotype Distribution Worldwide: Systematic Review and Meta-analyses. Clinical infectious diseases : an official publication of the Infectious Diseases Society of America. 2017;65:S112-S24.
7. Schuchat A. Epidemiology of Group B Streptococcal disease in the United States: shifting paradigms. Clinical microbiology reviews. 1998;11:497-513.
8. Edwards MS, Rench MA, Haffar AA, Murphy MA, Desmond MM, Baker CJ. Long-term sequelae of Group B Streptococcal meningitis in infants. The Journal of pediatrics. 1985;106:717-22.
9. Ohlsson A, Shah VS. Intrapartum antibiotics for known maternal Group B Streptococcal colonization. The Cochrane database of systematic reviews. 2014:CD007467.
10. Armistead B, Oler E, Adams Waldorf K, Rajagopal L. The Double Life of Group B *Streptococcus*: Asymptomatic Colonizer and Potent Pathogen. Journal of Molecular Biology. 2019;431:2914-31.
11. Curtis J, Kim G, Wehr NB, Levine RL. Group B Streptococcal phospholipid causes pulmonary hypertension. Proceedings of the National Academy of Sciences of the United States of America. 2003;100:5087-90.
12. Fischer W. The polar lipids of Group B Streptococci. II. Composition and positional distribution of fatty acids. Biochimica et biophysica acta. 1977;487:89-104.
13. Doran KS, Engelson EJ, Khosravi A, Maisey HC, Fedtke I, Equils O, et al. Blood-brain barrier invasion by Group B *Streptococcus* depends upon proper cell-surface anchoring of lipoteichoic acid. The Journal of clinical investigation. 2005;115:2499-507.

14. Slavetinsky C, Kuhn S, Peschel A. Bacterial aminoacyl phospholipids - Biosynthesis and role in basic cellular processes and pathogenicity. Biochimica et biophysica acta Molecular and cell biology of lipids. 2017;1862:1310-8.
15. Peschel A, Jack RW, Otto M, Collins LV, Staubitz P, Nicholson G, et al. *Staphylococcus aureus* resistance to human defensins and evasion of neutrophil killing via the novel virulence factor MprF is based on modification of membrane lipids with L-lysine. Journal of Experimental Medicine. 2001;193:1067-76.
16. Weidenmaier C, Peschel A, Kempf VA, Lucindo N, Yeaman MR, Bayer AS. DltABCD- and MprF-mediated cell envelope modifications of Staphylococcus aureus confer resistance to platelet microbicidal proteins and contribute to virulence in a rabbit endocarditis model. Infect Immun. 2005;73(12):8033-8.
17. Kuypers JM, Heggen LM, Rubens CE. Molecular analysis of a region of the Group B *Streptococcus* chromosome involved in type III capsule expression. Infection and immunity. 1989;57:3058-65.
18. Lancefield RC, McCarty M, Everly WN. Multiple mouse-protective antibodies directed against Group B Streptococci. Special reference to antibodies effective against protein antigens. The Journal of experimental medicine. 1975;142:165-79.
19. Wilkinson HW. Nontypable Group B Streptococci isolated from human sources. Journal of clinical microbiology. 1977;6:183-4.
20. Roy H, Ibba M. RNA-dependent lipid remodeling by bacterial multiple peptide resistance factors. Proceedings of the National Academy of Sciences of the United States of America. 2008;105:4667-72.
21. Deng L, Spencer BL, Holmes JA, Mu R, Rego S, Weston TA, et al. The Group B Streptococcal surface antigen I/II protein, BspC, interacts with host vimentin to promote adherence to brain endothelium and inflammation during the pathogenesis of meningitis. PLoS pathogens. 2019;15:e1007848.
22. Spencer BL, Deng L, Patras KA, Burcham ZM, Sanches GF, Nagao PE, et al. Cas9 contributes to Group B Streptococcal colonization and disease. Frontiers in Microbiology. 2019;10:1-15.
23. Faralla C, Metruccio MM, De Chiara M, Mu R, Patras KA, Muzzi A, et al. Analysis of two-component systems in group B Streptococcus shows that RgfAC and the novel FspSR modulate virulence and bacterial fitness. mBio. 2014;5(3):e00870-14.
24. Spencer BL, Chatterjee A, Duerkop BA, Baker CJ, Doran KS. Complete Genome Sequence of Neonatal Clinical Group B Streptococcal Isolate CJB111. Microbiology resource announcements. 2021;10.
25. Mu R, Cutting AS, Del Rosario Y, Villarino N, Stewart L, Weston TA, et al. Identification of CiaR Regulated Genes That Promote Group B Streptococcal Virulence and Interaction with Brain Endothelial Cells. PLoS One. 2016;11(4):e0153891.
26. Reichmuth AM, Oberli MA, Jaklenec A, Langer R, Blankschtein D. mRNA vaccine delivery using lipid nanoparticles. Ther Deliv. 2016;7(5):319-34.
27. Hafez IM, Maurer N, Cullis PR. On the mechanism whereby cationic lipids promote intracellular delivery of polynucleic acids. Gene Ther. 2001;8(15):1188-96.
28. Ernst CM, Kuhn S, Slavetinsky CJ, Krismer BB, Heilbronner S, Gekeler C, et al. The Lipid-Modifying Multiple Peptide Resistance Factor Is an Oligomer Consisting of Distinct Interacting Synthase and Flippase subunits. mBio. 2015;6:1-9.

29. Roy H, Ibba M. Broad range amino acid specificity of RNA-dependent lipid remodeling by multiple peptide resistance factors. Journal of Biological Chemistry. 2009;284:29677-83.
30. Hebecker S, Krausze J, Hasenkampf T, Schneider J, Groenewold M, Reichelt J, et al. Structures of two bacterial resistance factors mediating tRNA-dependent aminoacylation of phosphatidylglycerol with lysine or alanine. Proceedings of the National Academy of Sciences of the United States of America. 2015;112:10691-6.
31. Lennarz WJ, Nesbitt JA, Reiss J. The participation of sRNA in the enzymatic synthesis of O-L-lysyl phosphatidylgylcerol in *Staphylococcus aureus*. Proceedings of the National Academy of Sciences of the United States of America. 1966;55:934-41.
32. Saar-Dover R, Bitler A, Nezer R, Shmuel-Galia L, Firon A, Shimoni E, et al. D-alanylation of lipoteichoic acids confers resistance to cationic peptides in Group B *Streptococcus* by increasing the cell wall density. PLoS pathogens. 2012;8:e1002891.
33. Surve MV, Anil A, Kamath KG, Bhutda S, Sthanam LK, Pradhan A, et al. Membrane Vesicles of Group B *Streptococcus* Disrupt Feto-Maternal Barrier Leading to Preterm Birth. PLOS Pathogens. 2016;12:e1005816.
34. Van De Rijn I, Kessler RE. Growth characteristics of Group A Streptococci in a new chemically defined medium. Infection and Immunity. 1980;27:444-8.
35. Chang JC, LaSarre B, Jimenez JC, Aggarwal C, Federle MJ. Two Group A Streptococcal peptide pheromones act through opposing rgg regulators to control biofilm development. PLoS Pathogens. 2011;7:e1002190.
36. Gupta R, Shah P, Swiatlo E. Differential gene expression in *Streptococcus pneumoniae* in response to various iron sources. Microbial Pathogenesis. 2009;47:101-9.
37. Granok AB, Parsonage D, Ross RP, Caparon MG. The RofA binding site in *Streptococcus pyogenes* is utilized in multiple transcriptional pathways. Journal of bacteriology. 2000;182:1529-40.
38. Jeng A, Sakota V, Li Z, Datta V, Beall B, Nizet V. Molecular genetic analysis of a group A Streptococcus operon encoding serum opacity factor and a novel fibronectin-binding protein, SfbX. J Bacteriol. 2003;185(4):1208-17.
39. Hooven TA, Bonakdar M, Chamby AB, Ratner AJ. A Counterselectable Sucrose Sensitivity Marker Permits Efficient and Flexible Mutagenesis in *Streptococcus agalactiae*. Applied and environmental microbiology. 2019;85:1-13.
40. Holo H, Nes IF. High-frequency transformation, by electroporation, of *Lactococcus lactis* subsp. *cremoris* grown with glycine in osmotically stabilized media. Applied and Environmental Microbiology. 1989;55:3119-23.
41. Framson PE, Nittayajarn A, Merry J, Youngman P, Rubens CE. New genetic techniques for Group B Streptococci: High-efficiency transformation, maintenance of temperature-sensitive pWV01 plasmids, and mutagenesis with Tn917. Applied and Environmental Microbiology. 1997;63:3539-47.
42. Tan BK, Bogdanov M, Zhao J, Dowhan W, Raetz CRH, Guan Z. Discovery of a cardiolipin synthase utilizing phosphatidylethanolamine and phosphatidylglycerol as substrates. Proceedings of the National Academy of Sciences. 2012;109:16504-9.
43. Li C, Tan BK, Zhao J, Guan Z. In vivo and in vitro synthesis of phosphatidylglycerol by an *Escherichia coli* cardiolipin synthase. Journal of Biological Chemistry. 2016;291:25144-53.

566 44. Kim BJ, Hancock BM, Bermudez A, Del Cid N, Reyes E, van Sorge NM, et al. Bacterial
567 induction of Snail1 contributes to blood-brain barrier disruption. The Journal of clinical
568 investigation. 2015;125:2473-83.
569 45. Banerjee A, Kim BJ, Carmona EM, Cutting AS, Gurney MA, Carlos C, et al. Bacterial
570 Pili exploit integrin machinery to promote immune activation and efficient blood-brain
571 barrier penetration. Nature communications. 2011;2:462.

572

573

Figure legends

Fig 1. Lipidomic profiling of GBS and identification of Lys-Glc-DAG synthesized by MprF. Total ion chromatogram (TIC) of LC/MS in A) negative ion mode, B) positive ion mode shows a major unknown lipid eluting at ~25-29 min. C) Positive ESI/MS showing the $[M+H]^+$ ions of the unknown lipid. D) Positive ion MS/MS spectrum of $[M+H]^+$ at *m/z* 885.6 and E) negative ion MS/MS spectrum of $[M-H]^-$ at *m/z* 883.6 of the unknown lipid. F) Lys-Glc-DAG (16:0/18:1) is proposed as the structure of the unknown lipid. G) TIC showing loss of Lys-Glc-DAG and Lys-PG in COH1Δ*mprF* which is present when *mprF* is complemented *in trans*. H) Lys-Glc-DAG and Lys-PG is only present in *S. mitis* when expressing GBS *mprF* compared to Lys-PG only when expressing *E. faecium mprF*. "*" denotes methylcarbamate of Lys-Glc-DAG, an extraction artifact due to the use of chloroform. I) Biosynthetic pathways involving MprF.

Fig 2. Contribution of lysine lipids to meningitis pathogenesis. A) *In vitro* assays for adherence and invasion of hCMEC cells indicates *mprF* contributes to invasion but not adherence to brain endothelium (mean of 3 replicate experiments with 4 technical replicates, mean and SEM). B) pH-adjusted medium growth indicates Δ*mprF* cannot survive in low pH conditions, mean and SD. Groups of CD-1 mice were injected intravenously with COH1 WT or COH1Δ*mprF* strains and bacterial counts were assessed in the C) brain and D) blood after 72h. Representative data from 2 independent experiments are shown (WT, *n* = 20; Δ*mprF, n* = 19). E) Hematoxylin-eosin-stained brain sections from representative mice infected with WT (top) or Δ*mprF* mutant (bottom); arrows indicate meningeal thickening and leukocyte infiltration. F) Quantification of meningeal thickening using ImageJ. G) KC chemokine production measured by ELISA. Panels C, D, F, and G) median indicated. Statistical analyses performed using GraphPad Prism: A) One-way ANOVA with Tukey's multiple comparisons test; C, D, F) unpaired two-tailed t-test; G) Mann-Whitney U test; p-values indicated; ns, no significance (p-value > 0.05).

Supplemental files

Supplemental Figure S1. Detection of Lys-PG and Lys-Glc-DAG in *S. agalactiae* A909 and *S. agalactiae* CNCTC 10/84.

Supplemental Figure S2. Isotopic incorporation of deuterated lysine and ^{13}C-labeled glucose into Lys-Glc-DAG and Lys-PG.

Supplemental Figure S3. Positive ion mass spectra of retention time 27-29 minutes of hypervirulent CJB111 strain.

Supplemental Figure S4. *In vitro* hCMEC adhesion and invasion of CJB111 strains.

Supplemental Table S1. Observed and calculated exact masses of the $[M+H]^+$ ions of Lys-Glc-DAG molecular species in *S. agalactiae* COH1.

Supplemental Table S2. Strains and plasmids used in this study.

614 Supplemental Table S3. Primers used in this study.

615

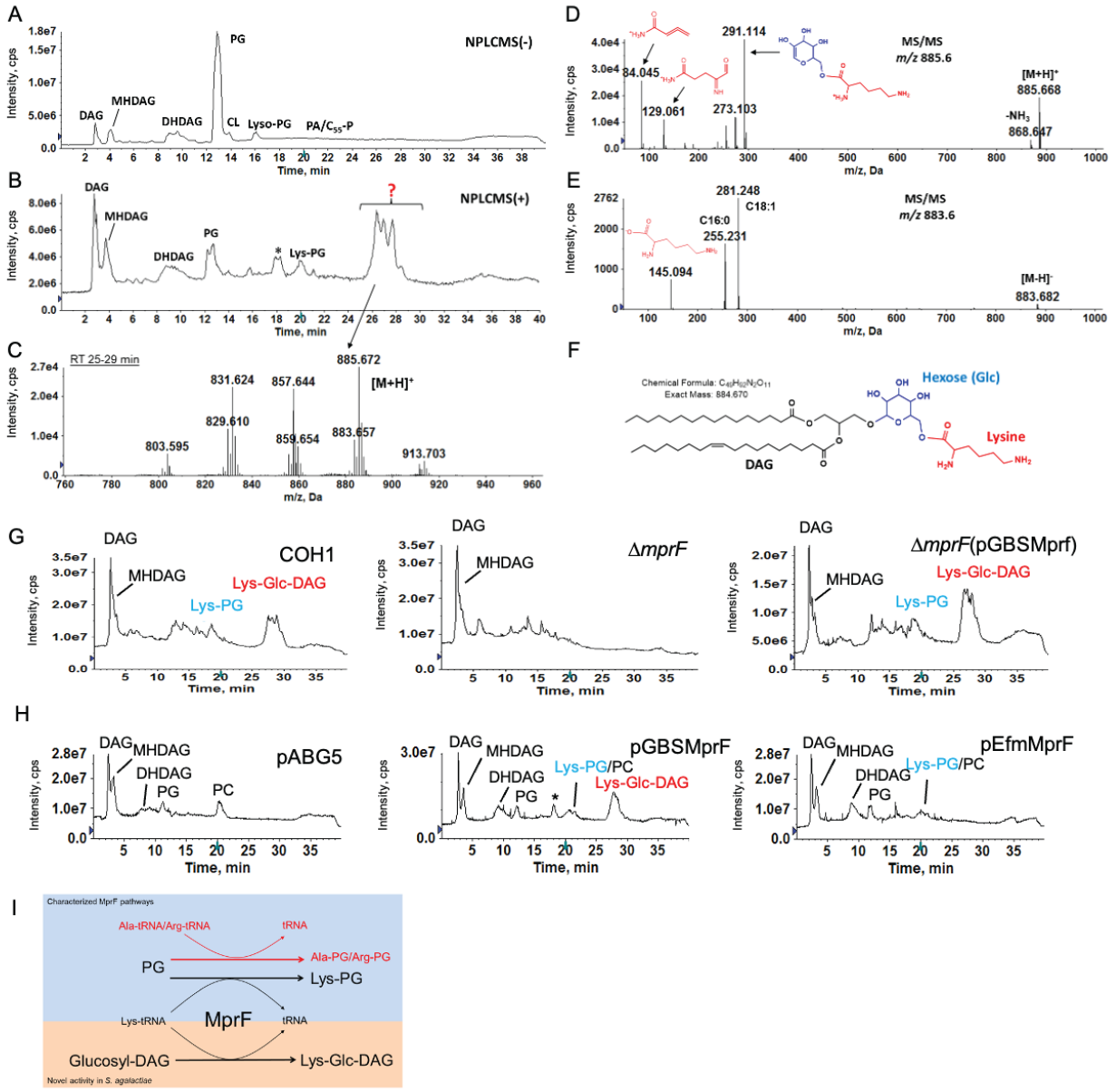

Fig 1. Lipidomic profiling of GBS and identification of Lys-Glc-DAG synthesized by MprF. Total ion chromatogram (TIC) of LC/MS in A) negative ion mode, B) positive ion mode shows a major unknown lipid eluting at ~25-29 min. C) Positive ESI/MS showing the $[M+H]^+$ ions of the unknown lipid. D) Positive ion MS/MS spectrum of $[M+H]^+$ at *m/z* 885.6 and E) negative ion MS/MS spectrum of $[M-H]^-$ at *m/z* 883.6 of the unknown lipid. F) Lys-Glc-DAG (16:0/18:1) is proposed as the structure of the unknown lipid. G) TIC showing loss of Lys-Glc-DAG and Lys-PG in COH1Δ*mprF* which is present when *mprF* is complemented *in trans*. H) Lys-Glc-DAG and Lys-PG is only present in *S. mitis* when expressing GBS *mprF* compared to Lys-PG only when expressing *E. faecium mprF*. "*" denotes methylcarbamate of Lys-Glc-DAG, an extraction artifact due to the use of chloroform. I) Biosynthetic pathways involving MprF.

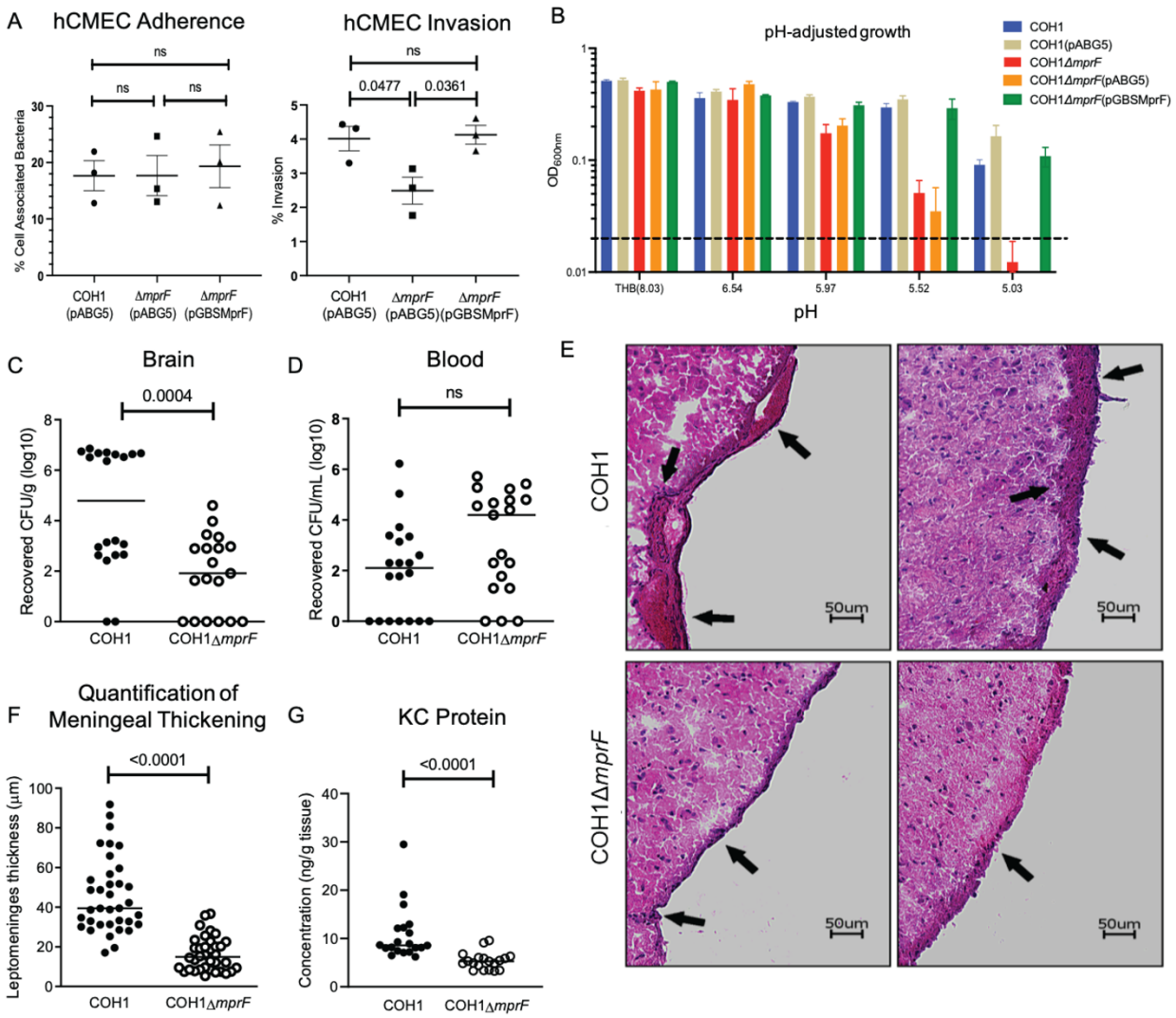

Fig 2. Contribution of lysine lipids to meningitis pathogenesis. A) *In vitro* assays for adherence and invasion of hCMEC cells indicates *mprF* contributes to invasion but not adherence to brain endothelium (mean of 3 replicate experiments with 4 technical replicates, mean and SEM). B) pH-adjusted medium growth indicates Δ*mprF* cannot survive in low pH conditions, mean and SD. Groups of CD-1 mice were injected intravenously with COH1 WT or COH1Δ*mprF* strains and bacterial counts were assessed in the C) brain and D) blood after 72h. Representative data from 2 independent experiments are shown (WT, *n* = 20; Δ*mprF, n* = 19). E) Hematoxylin-eosin-stained brain sections from representative mice infected with WT (top) or Δ*mprF* mutant (bottom); arrows indicate meningeal thickening and leukocyte infiltration. F) Quantification of meningeal thickening using ImageJ. G) KC chemokine production measured by ELISA. Panels C, D, F, and G) median indicated. Statistical analyses performed using GraphPad Prism: A) One-way ANOVA with Tukey's multiple comparisons test; C, D, F) unpaired two-tailed t-test; G) Mann-Whitney U test; p-values indicated; ns, no significance (p-value > 0.05).

644 **Supplemental Figures, and Tables**

645 **Identification of a novel cationic glycolipid in *Streptococcus agalactiae* that**

646 **contributes to brain entry and meningitis**

647

648 Luke R. Joyce[a], Haider S. Manzer[b], Jéssica da C. Mendonça[b,c], Ricardo Villarreal[b],
649 Prescilla E. Nagao[c] , Kelly S. Doran[b#,] Kelli L. Palmer[a#], and Ziqiang Guan[d#]

650

651 [a]Department of Biological Sciences, The University of Texas at Dallas, Richardson, TX,

652 75080

653 [b]Department of Immunology and Microbiology, University of Colorado School of

654 Medicine, Aurora, CO, 80045

655 [c]Rio de Janeiro State University, Roberto Alcântara Gomes Biology Institute, Rio de

656 Janeiro, RJ, Brazil

657 [d]Department of Biochemistry, Duke University Medical Center, Durham, NC, 27710

658

659

660 [#]Corresponding authors

661

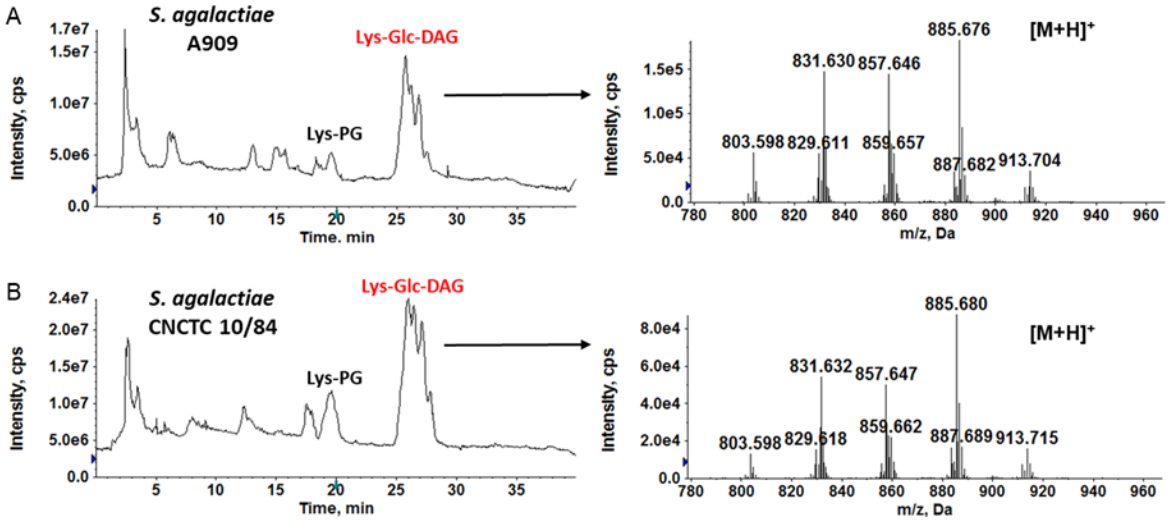

662

663 **Supplemental Figure S1. Detection of Lys-PG and Lys-Glc-DAG in *S. agalactiae***
664 **A909 and *S. agalactiae* CNCTC 10/84.** Positive TICs (left panels) showing the presence
665 of Lys-PG and Lys-Glc-DAG in S*. agalactiae* A909 and S*. agalactiae* CNCTC 10/84. Mass
666 spectra (right panels) show the $[M+H]^+$ ions of Lys-Glc-DAG.

667

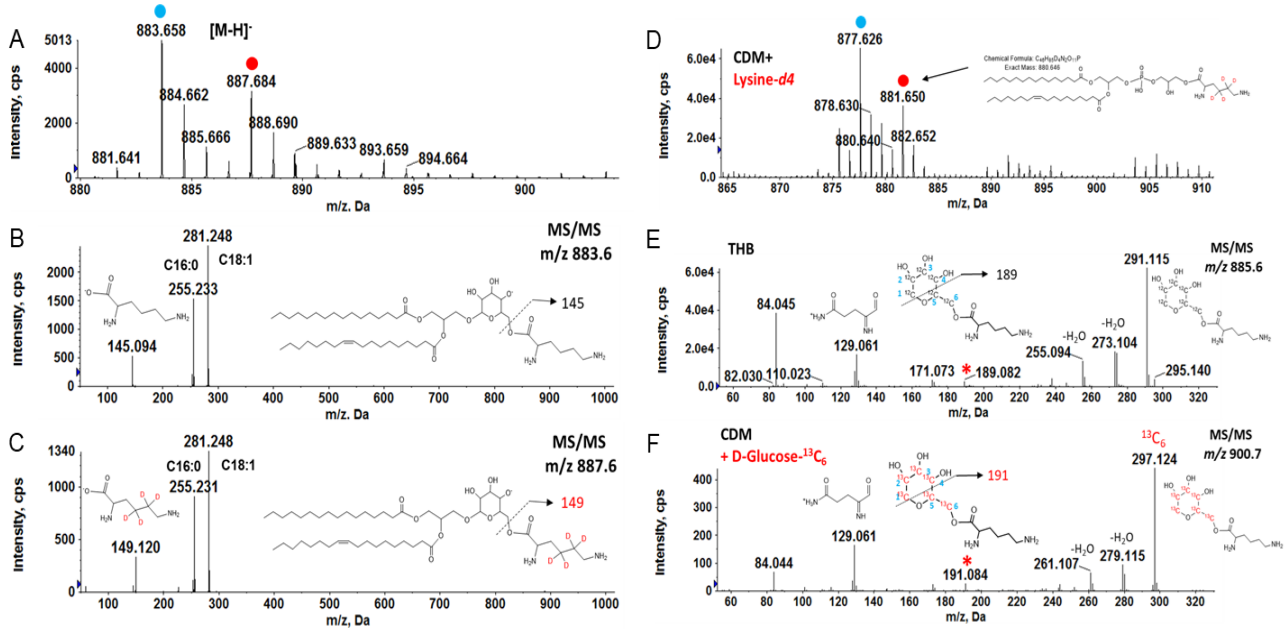

Supplemental Figure S2. Isotopic incorporation of deuterated lysine and ^{13}C-labeled glucose into Lys-Glc-DAG and Lys-PG. The lipid extracts of *S. agalactiae* COH1 cultured in DM, DM supplemented with 450 µM L-lysine-*d4* (4,4,5,5-D4), or in DM containing 0.5% w/v D-Glucose (U-$^{13}C_6$) were analyzed by LC-ESI/MS in the positive ion mode. A) Negative ESI/MS of $[M-H]^-$ ions of major Lys-Glc-DAG species in *S. agalactiae* COH1 when cultured in DM supplemented with lysine-*d4*. The incorporation of lysine-*d4* into Lys-Glc-DAG is evidenced by an upward *m/z* shift of 4 Da of the $[M-H]^-$ ion (from *m/z* 883 to *m/z* 887). B) MS/MS of $[M-H]^-$ at *m/z* 883.6 produces a deprotonated lysine residue at *m/z* 145. C) MS/MS of $[M-H]^-$ at *m/z* 887.6 produces a deprotonated lysine-*d4* residue at *m/z* 149. D) $[M+H]^+$ ions of major Lys-PG species in *S. agalactiae* COH1 cultured in DM supplemented with lysine-*d4.* The incorporation of lysine-*d4* in Lys-PG is evidenced by an upward *m/z* shift of 4 Da from unlabeled Lys-PG (blue dot) to labeled Lys-PG (red dot). E) MS/MS of 885.6. A major product ion at *m/z* 291.1 is derived from glucose-lysine residue. F) MS/MS of *m/z* 900.7 (containing fifteen ^{13}C atoms). The presence of *m/z* 297.1 (with 6 Da shift) is consistent with glucose in Lys-Glc-DAG is replaced with D-Glucose (U-$^{13}C_6$). The other nine ^{13}C atoms are incorporated into the DAG portion of Lys-Glc-DAG. Furthermore, MS/MS data indicate that lysine is linked to the C6 position of glucose by the fragmentation schemes for forming *m/z* 189 ion from the unlabeled Lys-Glc-DAG and *m/z* 191 ion from the ^{13}C-labeled Lys-Glc-DAG.

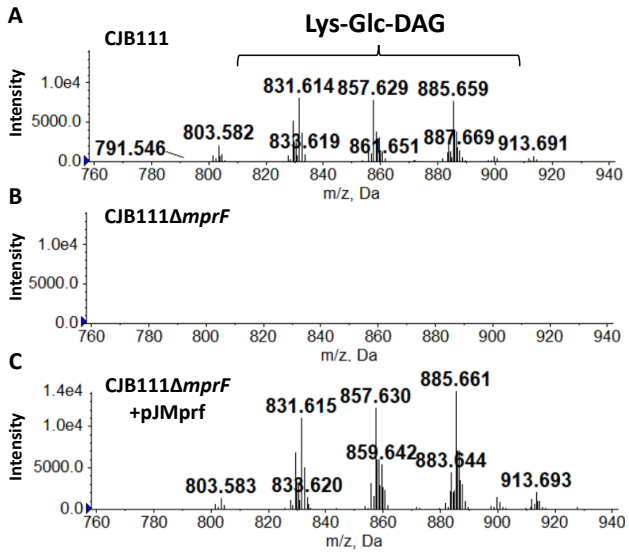

689

690 **Supplemental Figure S3. Positive ion mass spectra of retention time 27-29 minutes**
691 **of hypervirulent CJB111 strain.** Lys-Glc-DAG is present in the membrane of WT
692 CJB111 (A). Deletion of *mprF* from CJB111 genome results in loss of Lys-Glc-DAG from
693 the membrane (B). *MprF* complemented *in trans* reestablishes Lys-Glc-DAG back into
694 the membrane (C).

695

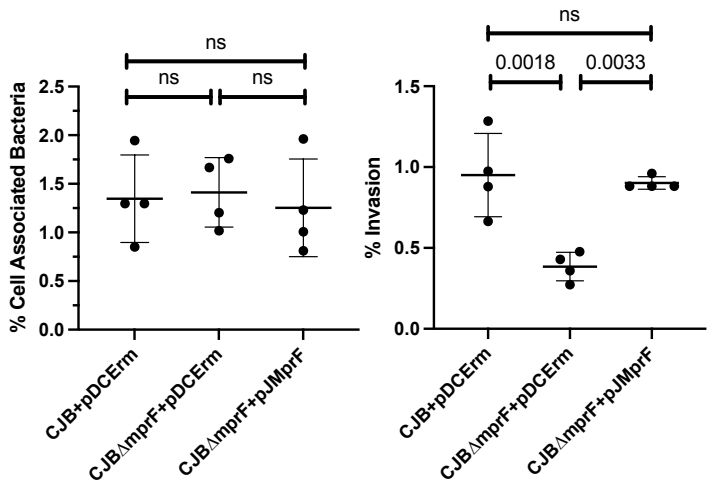

Supplemental Figure S4. *In vitro* hCMEC adhesion and invasion of CJB111 strains. *In vitro* assays for adherence and invasion of hCMEC cells indicates *mprF* contributes to invasion but not adherence to brain endothelium. Data indicates the percentage of the initial inoculum that was recovered. Experiments were performed three times with each condition in quadruplicate. Data from one representative experiment is shown, mean and standard deviation indicated. One-Way ANOVA with Tukey's multiple comparisons statistical test was used. P-values indicated; ns, not significant.

Supplemental Table S1. Observed and calculated exact masses of the $[M+H]^+$ ions of Lys-Glc-DAG molecular species in *S. agalactiae* COH1.

Lys-Glc-DAG[1]	$[M+H]^+$	
	Observed mass	Exact mass
C28:1	801.575	801.583
C28:0	803.595	803.599
C30:1	829.610	829.615
C30:0	831.624	831.630
C32:2	855.623	855.630
C32:1	857.644	857.646
C34:2	883.657	883.622
C34:1	885.672	885.677
C36:2	911.686	911.693
C36:1	913.703	913.709

[1]The numbers before and after colons indicate the total acyl chain carbon atoms and double bonds, respectively.

709 **Supplemental Table S2. Strains and plasmids used in this study.**

Organism	Strain	Description	Ref
S. agalactiae	ATCC BAA-1176 (COH1)	Wild-type *S. agalactiae* strain, serotype III	(1)
	COH1Δ*mprF*	*mprF* (GBSCOH1_1931) deletion strain	This work
	COH1Δ*mprF(*pABG5)	Empty vector control strain	This work
	COH1Δ*mprF*(pGBSMprf)	Expresses GBS *mprF* from P_{prtF} in pABG5Δ*phoZ*	This work
	COH1(pABG5)	Empty vector control	This work
	CJB111	Wilt-type *S. agalactiae* strain, serotype V	(2, 3)
	CJB111Δ*mprF*	*mprF* (ID870_10050) deletion strain	This work
	CJB111Δ*mprF*(pDCErm)	Empty vector control strain	This work
	CJB111Δ*mprF*(pJMprF)	Expresses GBS *mprF* in pDCErm	This work
	ATCC BAA-1138 (A909)	Wild-type *S. agalactiae* strain, serotype Ia	(4)
	CNCTC 10/84	Wild-type *S. agalactiae* strain, serotype V. Obtained from Dr. K Patras, UCSD	(5, 6)
S. mitis	ATCC 49456	Wild-type *S. mitis* type strain, also known as NCTC 12261	(7)
	ATCC 49456(pABG5)	Empty vector control	This work
	ATCC 49456(pGBSMprF)	Expresses GBS *mprF* from P_{prtF} in pABG5Δ*phoZ*	This work
	ATCC 49456(pEfmMprF1)	Expresses *E. faecium mprF1* from P_{prtF} in pABG5Δ*phoZ*	This work
	ATCC 49456(pEfmMprF2)	Expresses *E. faecium mprF1* from P_{prtF} in pABG5Δ*phoZ*	This work
E. coli	DH5α	Plasmid cloning host; F^-, φ80*lacZ*ΔM15, *rec*A1, *end*A1, *hsd*R17, *pho*A, *sup*E44, λ^- *thi*-1, *gyr*A96, *rel*A1	(8)
	DH5α(pABG5)	Empty vector control	This work
	MC1061	Plasmid cloning host; F^-, araD139, Δ(araABC-leu)7696, Δ(lac)X74, galU, galK, hsdR2, (r_K^- m_K^+), mcrB1, rpsL, (Str^r)	(9)

	MC1061(pDCErm)	Empty vector control	This work
	DH5α(pGBSMprF)	Expresses COH1 *mprF* (GBSCOH1_1931) from P_{prtF} in pABG5Δ*phoZ*	This work
	DH5α(pEfmMprF1)	Expresses *E. faecium mprF1* from P_{prtF} in pABG5Δ*phoZ*	This work
	DH5α(pEfmMprF2)	Expresses *E. faecium mprF1* from P_{prtF} in pABG5Δ*phoZ*	This work
	DH5α(pMBMprFKO)	Allelic exchange plasmid containing ~2 kb sequence flanking GBSCOH1_1931	This work
	MC1061(pJMprFKO)	Allelic exchange plasmid containing ~2 kb sequence flanking ID870_10050	This work
	MC1061(pJMprF)	Expresses CJB11 *mprF* from $P_{tetM/erm}$ in pDCErm	This work
E. faecium	1,231,410	Wild type *E. faecium* strain	(10)

Plasmid	**Description**	**Ref**
pABG5Δ*phoZ*	Constitutive expression vector for streptococci with the P_{prtF} promoter. Confers kanamycin resistance. Referred to as pABG5 throughout the text	(11)
pGBSMprF	pABG5Δ*phoZ* expressing COH1 *mprF* (GBSCOH1_1931) from P_{prtF}	This work
pEfmMprF1	pABG5Δ*phoZ* expressing *E. faecium* 1,231,410 *mprF1* (EFTG_00601) from P_{prtF}	This work
pMBSacB	Allelic exchange plasmid for *S. agalactiae*. Confers erythromycin resistance and sucrose sensitivity	(12)
pMBMprFKO	Knockout plasmid containing ~2 kb sequence flanking GBSCOH1_1931	This work
pJMprFKO	Knockout plasmid containing ~2 kb sequence flanking ID870_10050	This work
pDCErm	Consitituitive expression vector for streptococcus from $P_{tetM/erm}$	(13)
pJMprF	pDCErm expressing CJB111 *mprF* (ID870_10050)	This work

712 **Supplemental Table S3. Primers used in this study.**

Primer	5' – 3' sequence	Use
GBS_MprF_F	GAGAGGTCCCTTTCCTTGAAAAAGC TAATTGAAAAAGTC	Amplify GBSCOH1_1931 for Gibson assembly
GBS_MprF_R	ACCAATACCTTTATCTTATTTAACAA TCTTAATTTTACTATC	Amplify GBSCOH1_1931 for Gibson assembly
Faec_MprF1_F	GAGAGGTCCCTTTCCTTGTTAAAAA ATACCATACAATG	Amplify EFTG_00601 for Gibson assembly
Faec_MprF1_R	ACCAATACCTTTATCTTAATACTTTC TTCGTATCC	Amplify EFTG_00601 for Gibson assembly
MpF_SacII	ACGTCACCGCGGTTGAAAAAGCTAA TTGAAAAAGTC	Amplify CJB111 *mprF* ID870_10050 for ligation
MpR_BamHI	ACGTCAGGATCCTTATTTAACAATCT TAATTTTACTATC	Amplify CJB111 *mprF* ID870_10050 for ligation
pABG5-5'	GGAAAGGGACCTCTCTTCCTAAAC	Linearize pABG5Δ*phoZ* for Gibson assembly
pABG5-3'	GATAAAGGTATTGGTAAATAACAAA	Linearize pABG5Δ*phoZ* for Gibson assembly
Expression plasmid sequencing		
GBS_S1	GAATGGAATAATATAGTAGGCT	For sequencing pGBSMprF/pJMprF, amplifies with pABG5_Fup2/ pF
GBS_S2	GATTGTATCCCTTATTCC	For sequencing pGBSMprF/pJMprF, amplifies with GBS_S3
GBS_S3	CGATTCAATAGCTTCAC	For sequencing pGBSMprF/pJMprF, amplifies with GBS_S2
GBS_S4	GATAAAAGGCTCTACTGG	For sequencing pGBSMprF/pJMprF, amplifies with pABG5_FDwn/pR
pABG5_FDwn	CCAATAATAATGACTAGAGAAG	For pABG5 plasmid insert sequencing
pABG5_Fup2	CAAAAGGTTTCGACTTTTCACC	For pABG5 plasmid insert sequencing
EF1_S1	GAATAACGCTGATCAAAAGT	For sequencing pEfmMprF1, amplifies with pABG5_Fup2
EF1_S2	TGCCAAGAGAAATAGTC	For sequencing pEfmMprF1, amplifies with EF1_S3
EF1_S3	ACAATCTCTTCGCTTG	For sequencing pEfmMprF1, amplifies with EF1_S2
EF1_S4	CCAACTGTTCTTCTCCAA	For sequencing pEfmMprF1, amplifies with pABG5_FDwn
pF	AGCGCTAGGAGGAAAC	For pDCErm plasmid insert sequencing
pR	CCCATGCCATCTCCAATC	For pDCErm plasmid insert sequencing
GBSCOH1_1931 knockout plasmid construction, sequencing, and integration screening		
Mp1F_PstI	ACGTCACTGCAGTTCAATTAGCTTTT TCAACAATTTC	Amplifies upstream fragment from within GBSCOH1_1931/ID870_10050 leaving 6 codons, with Mp1R_XhoI
Mp1R_XhoI	ACGTCACTCGAGGCTGTTTATGGTG CTTTG	5' most primer of upstream fragment, amplifies with Mp1F_PstI
Mp2F_XbaI	ACGTCATCTAGAGAAAAGGCTAGAT TACGAAC	3' most primer of downstream fragment, amplifies with Mp2R_PstI
Mp2R_PstI	ACGTCACTGCAGGTTAAATAAGCTTT ATTTGGCA	Amplifies downstream fragment leaving 2 codons and stop codon of GBSCOH1_1931/ID870_10050, with Mp2F_XbaI
T7 promoter	TAATACGACTCACTATAGGG	Amplifies with MpS5F below to sequence plasmid, amplifies with T3 promoter for insert screening and plasmid presence
T3 promoter	AATTAACCCTCACTAAAGGG	Amplifies with MpS3R below, amplifies with T7 promoter for insert screening and plasmid presence
Int_F	GCTAATTGAACTGCAGGTTAAATAA G	Anneals at *mprF* knockout site, amplifies with Out_R for single integration screening

Out_R	GCTATTATATTTAGTGGTTTAATTGG	Anneals outside recombination arms, amplifies with Int_F, for single integration screening
Genomic knockout region sequencing		
MpS3F	CATTAGCTAGTCTTATCGGAG	Anneals outside integration arms, amplifies with MpS3R
MpS3R	ACAGCTACTTGGTAGTTCA	Amplifies with MpS3F
MpS4F	GCTACTAAGGCAAGATACG	Amplifies with MpS4R, knockout screening and plasmid sequencing primer
MpS4R	ATGGTCAGCGATGGTG	Amplifies with MpS4F, knockout screening and plasmid sequencing primer
MpS5F	CATAAGCGAAATAACTTGAG	Amplifies with MpS5R
MpS5R	GTATACAACGGCTTGATTGG	Anneals outside integration arms, amplifies with MpS5F

713

714

References

1. Kuypers JM, Heggen LM, Rubens CE. Molecular analysis of a region of the Group B *Streptococcus* chromosome involved in type III capsule expression. Infection and immunity. 1989;57:3058-65.
2. Faralla C, Metruccio MM, De Chiara M, Mu R, Patras KA, Muzzi A, et al. Analysis of two-component systems in group B Streptococcus shows that RgfAC and the novel FspSR modulate virulence and bacterial fitness. mBio. 2014;5(3):e00870-14.
3. Spencer BL, Chatterjee A, Duerkop BA, Baker CJ, Doran KS. Complete Genome Sequence of Neonatal Clinical Group B Streptococcal Isolate CJB111. Microbiology resource announcements. 2021;10.
4. Lancefield RC, McCarty M, Everly WN. Multiple mouse-protective antibodies directed against Group B Streptococci. Special reference to antibodies effective against protein antigens. The Journal of experimental medicine. 1975;142:165-79.
5. Hooven TA, Randis TM, Daugherty SC, Narechania A, Planet PJ, Tettelin H, et al. Complete Genome Sequence of *Streptococcus agalactiae* CNCTC 10/84, a Hypervirulent Sequence Type 26 Strain. Genome announcements. 2014;2:e01338-14.
6. Wilkinson HW. Nontypable Group B Streptococci isolated from human sources. Journal of clinical microbiology. 1977;6:183-4.
7. Kilian M, Mikkelsen L, Henrichsen J. Taxonomic Study of Viridans Streptococci: Description of *Streptococcus gordonii* sp. nov. and Emended Descriptions of *Streptococcus sanguis* (White and Niven 1946), *Streptococcus oralis* (Bridge and Sneath 1982), and *Streptococcus mitis* (Andrewes and Horder 1906). International Journal of Systematic Bacteriology. 1989;39:471-84.
8. Taylor RG, Walker DC, Mclnnes RR. *E. coli* host strains significantly affect the quality of small scale plasmid DNA preparations used for sequencing. Nucleic acids research. 1993;21:1677-8.
9. Casadaban MJ, Cohen SN. Analysis of gene control signals by DNA fusion and cloning in Escherichia coli. J Mol Biol. 1980;138(2):179-207.
10. Palmer KL, Carniol K, Manson JM, Heiman D, Shea T, Young S, et al. High-quality draft genome sequences of 28 *Enterococcus* sp. isolates. Journal of bacteriology. 2010;192:2469-70.
11. Granok AB, Parsonage D, Ross RP, Caparon MG. The RofA binding site in *Streptococcus pyogenes* is utilized in multiple transcriptional pathways. Journal of bacteriology. 2000;182:1529-40.
12. Hooven TA, Bonakdar M, Chamby AB, Ratner AJ. A Counterselectable Sucrose Sensitivity Marker Permits Efficient and Flexible Mutagenesis in *Streptococcus agalactiae*. Applied and environmental microbiology. 2019;85:1-13.
13. Jeng A, Sakota V, Li Z, Datta V, Beall B, Nizet V. Molecular genetic analysis of a group A Streptococcus operon encoding serum opacity factor and a novel fibronectin-binding protein, SfbX. J Bacteriol. 2003;185(4):1208-17.